Unlocking the potential of remote sensing for kelp biomass estimation in South African Kelp Concession Areas

Lauren Jane Searle

(SRLLAU001)

Department of Biological Sciences

University of Cape Town

Rondebosch, Cape Town

South Africa

Supervisors: John Bolton, Mark Rothman, Kate Bray

June 2024

Dissertation submitted in partial fulfilment of the requirements for the degree of Master of Science (by coursework and dissertation) in Applied Ocean Sciences, through the Marine and Antarctic Research centre for Innovation and Sustainability (MARiS), in the Department of Biological Sciences, at the University of Cape Town

Plagiarism Declaration

I, Lauren Jane Searle, hereby:

1. grant the University of Cape Town free license to reproduce the above thesis in whole or in part, for the purpose of research;

2. declare that:

   (a) this dissertation is my own unaided work, both in concept and execution, and apart from the normal guidance from my supervisor, I have received no assistance except as acknowledged.
   (b) neither the substance nor any part of the above dissertation has been submitted in the past, or is being, or is to be submitted for a degree at this University or at any other university.

Signed by candidate

Lauren Jane Searle

Department of Biological Sciences
University of Cape Town

Wednesday 12 June, 2024

Abstract

The use of high-resolution imagery (HRI) has the potential to improve the accuracy of kelp biomass estimates, ensuring the implementation of sustainable harvesting. However, definitive research on the potential of HRI in this application is lacking in the current literature. An accurate estimation of kelp biomass is crucial to calculate maximum sustainable yield (MSY) in South African kelp Concessions. This study seeks to fill the knowledge gap by exploring the effectiveness of HRI for estimating the biomass of kelp along a specific stretch of coastline. The study aim is achieved by analysing HRI of Concession Area 6 taken from an aircraft. Maps quantifying kelp extent are derived from image classification methods applied to the HRI. A total biomass figure is then determined using the product of the calculated kelp extent and an average biomass figure of 14.5 kg/m^{-2}, taken from the literature. A total biomass of 40527.9 tonnes wet weight was calculated for Concession Area 6. The classification of HRI provided an overall accuracy of 95%, which is relatively high when compared to Sentinel-2 satellite imagery which resulted in an overall accuracy of 75%. When compared to the kelp extent measured in previous studies, HRI-derived maps had consistently less kelp coverage than maps from other imagery, suggesting that other imagery overestimates kelp extent (likely due to resolution). However, this was confounded given different imagery used at different times and so it was not possible to rule out change in kelp coverage over time. The results demonstrate the value of HRI in the mapping of kelp extent, which can ultimately be used to produce more accurate MSY assessments and support sustainable harvesting practices. However, before HRI can be integrated into MSY assessments, it is imperative to calculate more accurate biomass figures that are specific to the Concession Area, rather than relying on region wide estimates. Additionally, it's important to acknowledge that while HRI excels in precision, other imagery may be more suitable for large-scale estimates where accuracy is not a primary concern and due to its cost-effectiveness.

Keywords: High-resolution imagery, *Ecklonia maxima,* GIS, kelp mapping

Acknowledgements

To my family, who always comes first, I would like to express my heartfelt gratitude for your persistent support throughout the journey of completing this thesis. Your love and understanding have been invaluable.

I extend my sincere appreciation to my friends, especially my classmates, whose companionship and encouragement have been a source of inspiration. Your positivity has made this academic pursuit more enjoyable.

A special acknowledgment goes to Alex for your continuous support and being a reliable sounding board for the continuous exchange of ideas.

I would also like to express my gratitude to Taurus Chemicals Cape Kelp (Pty) Ltd for their collaboration and support in facilitating my research in Concession Area 6. Your cooperation has been instrumental in the success of this project.

I am deeply thankful to my supervisors, John Bolton, Mark Rothman, and Kate Bray, for their guidance, expertise, and unwavering support. Your mentorship has played a crucial role in shaping this thesis and my academic growth. I feel incredibly fortunate to have had the opportunity to work under your supervision, benefiting not only from your knowledge but also from the enriching experience you have provided throughout this academic journey.

To everyone who has contributed to my academic journey, thank you for being an integral part of this dissertation.

Table of contents

List of figures

List of tables

List of symbols/abbreviations

ANOVA-	Analysis of Variance
CSIR -	Council for Scientific and Industrial Research
DFFE –	Department of Forestry, Fisheries and Environment
ESA-	European Satellite Agency
GNSS -	Global Navigation Satellite System
IMU -	Inertial measurement unit
NIR –	Near- infrared
GPS -	Global Positioning System
HRI –	High-resolution imagery
LiDAR -	Light Detection and Ranging
MARiS -	Marine and Antarctic Research centre for Innovation and Sustainability
MLC –	Maximum Likelihood Classification
MSY -	Maximum Sustainable Yield
NDVI -	Normalized difference vegetation index
RS –	Remote Sensing
S-2 –	Sentinel-2
SAEON -	South African Environmental Observation Network
SRCA –	Seaweed Rights Concession Areas
UAV –	Unmanned aerial vehicle

1. Introduction

1.1. Kelp forests

Kelp forests are three-dimensional benthic seascape structures formed by seaweeds (Wernberg & Filbee-Dexter, 2019). The term ‘kelps’ is sometimes used in literature to describe large brown algae from different orders (Bolton, 2016). To avoid confusion, the term ‘kelp’ is used in this paper only to describe members of the order Laminariales.

Kelp forests construct their local environment to support distinct subtidal communities of plants and animals, which would not persist without the seaweed canopy (Wernberg & Filbee-Dexter, 2019). Kelp forests dominate the temperate nearshore reefs on approximately 25% of the coastlines globally. They are among Earth’s most productive primary producers, with a productivity per unit area equivalent to that of tropical rainforests (Blamey & Bolton, 2018). Kelps rely on photosynthesis for growth; therefore, their distribution and depth are greatly influenced by the availability of light (Anderson et al., 2006).

Kelp forests provide essential ecological services in shallow subtidal areas and adjacent deep-sea ecosystems (Blamey & Bolton, 2018; Filbee-Dexter & Wernberg, 2018). These forests are crucial as nursery grounds and provides a food source for many species (Anderson et al., 2006). Their large size, structure, physiology, and association with other organisms play a vital role in constructing the surrounding environment. Consequently, kelps are often referred to as ecosystem engineers ((Teagle et al., 2017; Miller et al., 2018)). For instance, kelp forests can modify the chemistry of seawater by taking up carbon and increasing pH and dissolved oxygen levels. They create physical gradients in carbon content, alkalinity, pH, and oxygen in water in their proximity, which is sustained by kelp density (Kosek & Kukliński, 2023). Kelp forests control water flow and sediment dynamics by reducing turbulence below the canopy. They also may diminish the wave force by absorbing some of the wave’s energy, reducing its velocity.

Therefore, they can act as a coastal buffer, dampening the impact of storms and extreme waves, thus preventing excessive sedimentation and coastal squeeze (Smale et al., 2013). Additionally, it's worth noting that kelps are also harvested for commercial use, adding another dimension to their ecological significance.

The standard structure of kelps consist of a holdfast, flexible stipe, and fronds. These three structures provide distinct functional habitat types (Teagle et al., 2017). The holdfast usually is comprised of intertwined haptera which anchor the sporophyte to the substratum (Elston, Anderson & Price, 2015). This structure provides an intricate temporal habitat for kelp recruits, other seaweeds, and many invertebrates (Field et al., 1980; Steneck et al., 2002; Teagle et al., 2017). Amongst kelp species, stipes vary in shape and size, including length, diameter, plasticity, rigidity, and the presence of branches (Rothman et al., 2015; Teagle et al., 2017). This structure provides a foundation for secondary habitat-forming species such as epiphytes and some fauna such as limpets (Anderson et al., 2006). The fronds are the primary photosynthetic organs and vary in shape and size depending on the species. For instance, some species have fronds that are categorised into primary blades and secondary blades that grow from the basal meristem (Rothman et al., 2017). The fronds can be colonised by a range of epibionts that impact the settlement of the associated biodiversity, i.e., the epiflora and epifauna (Anderson et al., 2006; Teagle et al., 2017).

1.2.South African kelp

South African kelp forests comprise of four species. These are *Ecklonia maxima* (Osbeck) Papenfuss*, Laminaria pallida* Greville ex J. Agardh*, Ecklonia radiata* (C. Agardh) J. Agardh and *Macrocystis pyrifera* Bory (Anderson et al., 2007; Rothman et al., 2015). The dominant species, *E. maxima* grows up to 15m and is commonly termed “sea bamboo” (Bolton et al., 2012). It has a long hollow stipe with a gas-filled bulb ending in the kelp head which consists

of a spearhead-shaped primary blade and secondary fronds, that grow laterally from the primary blade. The gas-filled bulb suspends the kelp head at or near the surface, making it visible during low tide (Rothman et al., 2010). *E. maxima* is termed a 'surface-reaching kelp' as it typically floats within the upper meter of the water column during high tides, or at (or above) the surface at low tide.. The presence of a head is dissimilar to some other kelp species, such as *M. pyrifera,* which has a continuous canopy of fronds forming a surface canopy (Gendall et al., 2023).

E. maxima dominates the waters on the west coast of South Africa, forming extensive kelp forests to depths between 5 – 10m (Bolton, 2010). The distribution of this species extends from just north of Luderitz, Namibia, south along the west coast of South Africa to just beyond the biogeographical break at Cape Agulhas, South Africa. (Rothman et al., 2020). Its distribution range is defined by water temperatures. The warmest monthly mean temperatures *E. maxima* is exposed to typically range from 13°C to 19°C, while the coldest temperatures range from 11°C to 14°C. Temperatures greater than 22.5°C limit the distribution of this kelp species (Bolton et al., 2012). On the South Coast of South Africa, *E. maxima* shifted 73km eastward in 2006 and has since been established in the De Hoop Nature Reserve. Bolton et al. (2012) hypothesised that this shift is restricted by aspects of the inshore water temperature regime; contemporary data suggesting that gradual cooling along this coast may have caused the change in distribution.

1.3.Kelp harvesting

In South Africa, most of the kelp industry focuses on harvesting *Ecklonia maxima* and *Laminaria pallida* (Anderson et al., 2006; Rothman, Anderson & Smit, 2006). Fresh kelp is harvested along the coastline between Port Nolloth (just south of the Namibian border) and Buffeljags (just west of Cape Agulhas), with the highest quantities being harvested in the

Western Cape. This stretch of coastline is divided into 23 Seaweed Rights Concession Areas (SRCAs) (Figure 1.1), 14 of which contain sufficient kelp for possible utilisation (Rothman et al., 2020). Currently, rights are allocated for a period of 15 years. In these SRCAs, rightsholders utilise one of two harvesting methods. The "lethal" technique involves killing the plant as the entire kelp head is cut off above the bulb at the top of the stipe (Levitt et al., 2002). The "non-

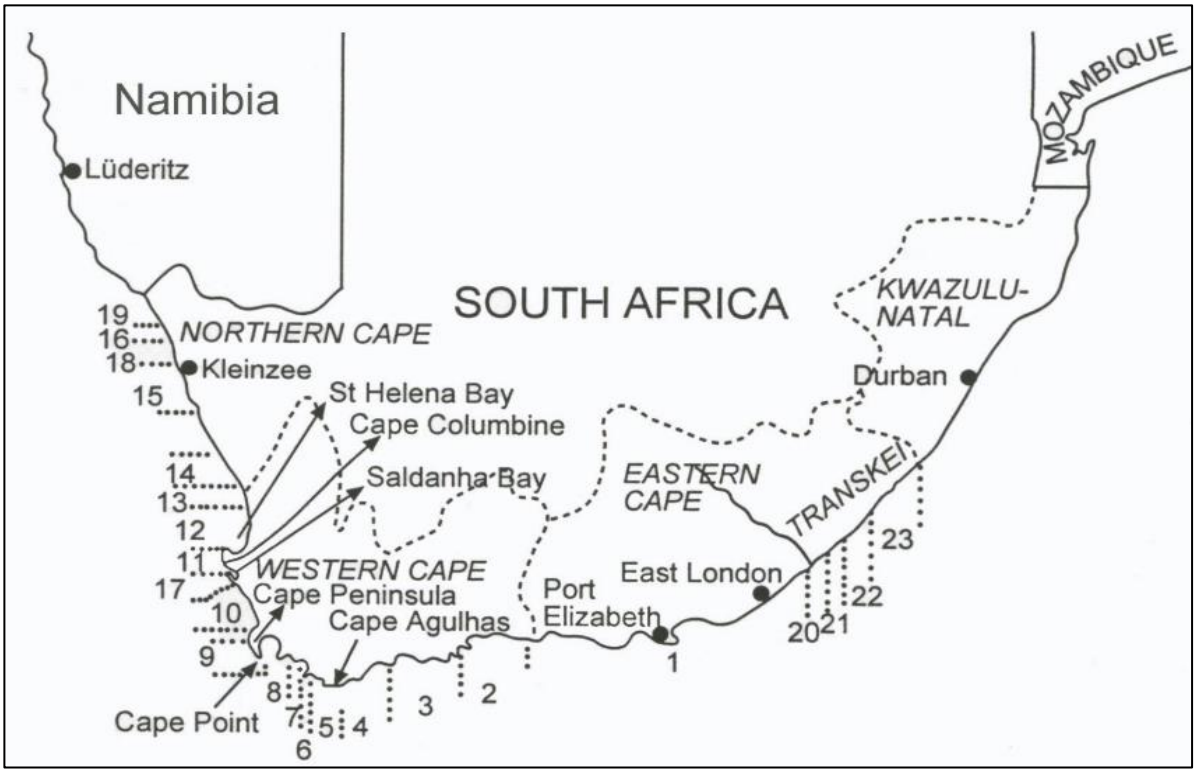

Figure 1.1. A map indicating the 23 Seaweed Rights Concession Areas on the South African coast. Areas 5–9, 11–16 and 18–19 contain kelp rights. Taken from Rothman et al. (2020).

lethal" method requires only removing the secondary fronds by cutting them 20cm above their junction with the primary blade. The non-lethal method keeps the meristems intact, allowing fronds to re-grow (Rothman et al., 2020).

The exploitation of kelps in South Africa was initially restricted to the collection of beach-cast kelp, which was exported for alginate production. In the 1970s, the first plant growth stimulant product was produced from *E. maxima* (Blamey & Bolton, 2018). Initially, only small amounts of fresh kelp were harvested commercially from kelp forests in South Africa. However, the markets for this product continue to expand, increasing the demand for fresh kelp harvesting.

Since the mid-1990s, there has been a rapid increase in shore-based abalone farming, leading to a corresponding increase in demand for fresh kelp for abalone feed (Anderson et al., 2007). Currently, the kelp industry uses 5766 tonnes of fresh kelp fronds for abalone feed, and 5194 tonnes of fresh whole kelp for the manufacturing of liquid fertilisers and stimulants (BSASA, 2023). According to the current trend, kelp harvested for plant growth is expected to overtake the kelp harvested for abalone feed (Rothman et al., 2020).

To ensure that harvesting remains sustainable, the Department of Forestry, Fisheries, and the Environment (DFFE) sets limits on the amount of kelp that can be harvested in SRCAs. These limits, also known as Maximum Sustainable Yield (MSY), allow right holders to harvest 10% of the estimated kelp biomass of the Concession Area (Rothman et al., 2020). However, setting an MSY has proven difficult due to unavailable or inaccurate estimates of kelp biomass, often the result of incomplete kelp forest maps (Anderson et al., 2007).

1.4. Estimating the total biomass of kelp forests

Accurate information on the biomass of kelp beds in a Concession Area is necessary for determining the MSY (Rothman et al., 2010). This enables better management of the kelp beds and reduces the potential for over-harvesting. Estimating the total kelp biomass of a Concession Area relies on two pieces of information. Firstly, a measurement of the average biomass of kelp specific to the Concession Area (per m^2). Secondly, a measurement of the area of the kelp forest within the Concession Area. The product of these two measurements provides an estimate of the total biomass of the kelp forest. The only published biomass estimate of surface-reaching kelp beds on the South African West Coast is greater than 593,000 t (Anderson et al., 2007).

1.5.Average kelp biomass estimation methods

Conventionally, in South Africa, estimating the average kelp biomass relied on sampling kelp in a series of $1m^2$ bottom quadrats, usually placed along a transect running perpendicular to the

shoreline (Field et al., 1980; Levitt et al., 2002; Anderson et al., 2006; Rothman et al., 2010). The kelp in the quadrats is removed and weighed, a method referred to as destructive bottom sampling. This method is highly labour-intensive. Using this method Rothman (2006), estimated the average kelp biomass for the Cape Peninsula and West Coast to be 14.5 kg/m^2. Surface-reaching plants constituted 62% of this kelp biomass figure, with subsurface kelp accounting for the remaining 38%. However, this average varied between study sites with the lowest biomass figure of 10 kg/m^2 at shallower sites and the highest biomass 21.3 kg/m^2 at deeper sites.

Subsequently, Rothman et al. (2010) determined a more accessible, quicker technique of estimating kelp biomass to avert destruction and speed up measurements. They used 1m^2 floating quadrats to establish correlations between the density of kelp heads at the water surface during low spring tides and total kelp biomass below the quadrat. They found a direct correlation between the number of kelp heads at the surface and kelp biomass. These surface density measurements are more than eight times quicker than the traditional biomass determination method, are non-destructive, and are unaffected by water clarity.

1.6. Kelp forest area measurements

Over extensive coastal areas, mapping kelp forests via a boat can be logistically challenging and resource-intensive due to often remote stretches of coastline and inaccessibility of kelp beds. Even when resources are available, these ground surveys produce spatially scattered data that has to be extrapolated over large areas (Bennion et al., 2019). Consequently, remote sensing (RS) is the only sensible way of estimating the area of kelp forests in Concession Areas and over large extents of the coast (Anderson et al., 2007). In South Africa, kelp forests have been previously mapped using RS data such as Landsat Satellite imagery (Anderson et al., 2007), infrared imagery taken from a plane (Tarr, 1993), and using Sentinel-2 satellite imagery (Dunga, 2019).

Remote sensing is the process of using technology to collect data without physical or direct contact with the object being studied ((Lillesand, Kiefer & Chipman, 2015)). RS employs various platforms and sensors to capture images and measurements of the Earth's features (Lillesand et al. 2015). For instance, RS can capture ocean data through satellites with multispectral sensors, light detection and ranging (LiDAR) devices, aerial cameras on aircraft and drones, underwater imagery via autonomous underwater vehicles (AUVs), and by using sound navigation and ranging SONAR on ships (Bennion et al., 2019).

The use of RS has enabled the capture of comprehensive and accurate information, most notably from regions that are difficult to access (Chen et al., 2022). Additionally, the imagery captured can be reacquired at a later stage, thus allowing users to conduct future surveys with minimal spatial variation (Lillesand et al. 2015). This enables researchers to collect seasonal to multi-decadal time-series data over large spatial scales (Bell, Cavanaugh & Siegel, 2015). Consequently, RS provides a practical instrument for the long-term monitoring of spatially extensive kelp forests (Sagawa et al., 2012; Mishra & Gould, 2016).

Environmental variables such as tidal height, wave power and ocean current can alter the amount of kelp visible on the days of data capture. Several studies have shown that the extent of kelp forests mapped is highly sensitive to tides and currents (Stekoll, Deysher & Hess, 2006; Nijland, Reshitnyk & Rubidge, 2019; Cavanaugh, Cavanaugh, et al., 2021). For example, Cavanaugh et al. (2021) estimated a 32% decrease in canopy area associated with a 0.1 m/s increase in current velocity. Additionally, Nijland et al. (2019) found that with a 2m increase in tide, there was a 40% decrease in kelp canopy mapped from satellite imagery. For surface-reaching kelps that are visible at the surface during low tides, such as *Ecklonia maxima*, mapping is usually based on satellite or aerial imagery taken at low spring tides (Anderson et al., 2007; Dunga, 2019).

1.7.Satellite imagery

Earth Observation satellites offer continuous worldwide coverage from several multispectral sensors (Bennion et al., 2019). These multispectral sensors can capture data across multiple parts of the electromagnetic spectrum. This includes visible (red, green and blue), near infrared, and shortwave infrared wavelengths, thus enabling the unique spectral signatures associated with chlorophyll absorption in photosynthetic organisms to be captured (Lillesand, Kiefer & Chipman, 2015). These multispectral sensors can be used to monitor kelp canopy dynamics across extensive areas. However, the type of satellite imagery used governs the imagery's temporal coverage and pixel resolution (Cavanaugh, Bell, et al., 2021). Often, freely available satellite imagery has a low resolution, which is often insufficient for accurate mapping of kelp beds. For instance, Deysher (1993) found that Satellite Pour l'Observation de la Terre (SPOT) satellite imagery with a spatial resolution of 20m was inadequate to map Californian *Macrocystis* beds accurately. Similarly, Stekoll et al. (2006) noted that Landsat imagery with a 15m resolution overestimated the size of kelp canopies in Alaska. Consequently, very high-resolution imagery, such as imagery with a pixel resolution less than 3m, is desirable when mapping intertidal kelps.

Hyperspectral imagery has been used previously to estimate kelp biomass and physiological conditions (Bell, Cavanaugh & Siegel, 2015). It has also been used to successfully map submerged seaweeds in Germany down to a depth of 6m (Uhl, Bartsch & Oppelt, 2016). The depth to which kelp can be mapped depends on the water clarity (Cavanaugh, Bell, et al., 2021). However, satellites that produce multispectral images with a resolution of up to 4m are often unaffordable for mapping large areas. Additionally, images must be captured at low tides, without cloud cover, and during good sea conditions, which is hard to align with the predetermined satellite path (Anderson et al., 2007).

An excellent example of freely available satellite imagery previously used by Dunga (2019) to map South African kelp beds is Sentinel-2 (S-2). S-2 is a satellite operation conducted by the European Space Agency (ESA). This operation consists of two identical satellites, S-2 A and 2B, equipped with a multispectral imaging system designed to capture high-resolution (up to 10m) optical images of the Earth's surface in different spectral bands (see Appendix A for a summary of the S-2 multispectral imagery spectral bands). The S-2 satellites provide global coverage with a revisit time of 5 days. This satellite imagery is open-access and designed for a wide range of applications, such as land cover mapping and monitoring, environmental management, and disaster response.

1.8.Aerial imagery

Aerial imagery captured by aircraft or unmanned aerial vehicles (UAVs) is the most adaptable method for controlling flight times and environmental variables (Cavanaugh, Bell, et al., 2021). Additionally, depending on the altitude of the flight, high-resolution imagery (HRI) can be captured, allowing for discrimination between species (Murfitt et al., 2017; Nahirnick et al., 2019). Cavanaugh et al. (2021) used UAVs to map and estimate the biomass canopies of *Macrocystis pyrifera* in California. However, this method is limited to areas of small spatial coverage, especially when using UAVs due to battery and flight time constraints.

1.9. Image classification

Once the satellite or aerial imagery has been collected, it can be analysed using image classification. Supervised image classification involves classifying an image into several predefined classes. The aim is to train a machine learning algorithm to recognise features in an image that distinguish one class from another. These classes can represent objects or pixels (Lillesand, Kiefer & Chipman, 2015). This method allows the classification algorithm to distinguish and classify vegetation in an image, such as kelp, from other elements, such as

water or rocks (Al-doski et al., 2013). The classification of kelp can then be used to derive information such as biomass, spatial trends, and temporal change (St-Pierre & Gagnon, 2020). Although aerial imagery has been successfully implemented in detecting and mapping floating seaweed communities, sun glare, clouds, crashing waves, shadows, and spectral noise can hinder image classification (Cavanaugh et al., 2021).

1.10. Previous studies of remote sensing in South Africa

In South Africa, only a few studies have focused on mapping and monitoring kelp forest ecosystems. These studies include the Master of Science theses of Tarr (1993), Rand (2006), and Dunga (2019). Additionally, studies were done by Anderson et al. (2007), which included Rand's remote sensing data (2006), and by CSIR (2022) to study the feasibility of kelp cultivation.

To quantify abalone habitat, Tarr (1993) created hard copy maps illustrating the distribution of kelp across Concession Areas 5, 6, 7, 8, and Dyer Island using infrared aerial photography. Subsequently, Anderson et al. (2007) digitised Tarr's maps and used Landsat 7 ETM+ satellite imagery and physical mapping with a GPS to map kelp beds. They estimated the biomass of these beds using the product of the average kelp biomass per m^2 (14.5 ± 1.33 kg/m^2 determined by Rothman (2006)) and the area of the kelp bed. Consequently, Anderson et al. (2007) established a coastal kelp resource database for the South African Coastline. More recently, Dunga (2019) aimed to update the South African kelp forest maps using Sentinel-2 satellite imagery. A total of 1300 km of kelp forest was mapped, distinguishing three biogeographical subtypes: the Namaqua, Cape, and Agulhas Kelp Forests. This new map was then used to facilitate the first ecosystem threat status assessment for South African kelp forests. In 2022, CSIR conducted a GIS study between Alexander Bay and Cape Agulhas on the West Coast to assess the potential offshore areas for kelp cultivation (CSIR, 2022). The study focused on

analysing GIS datasets of essential environmental requirements for kelp growth to distinguish regions where kelp farming is biologically viable from those where it is not feasible.

1.11. Study aim

Kelp rightsholders rely on accurate estimates of kelp biomass within their Concession Areas to ensure the implementation of sustainable business practices (Anderson et al., 2007). High-resolution imagery (HRI) has the potential to provide such estimates as an efficient means of capturing this information. Current literature is lacking in definitive research on the potential of HRI in this application. This study seeks to fill this knowledge gap by determining the effectiveness of HRI for the purpose of determining the maximum sustainable yield in South African SRCAs. This study's aim is achieved by analysing aerial imagery of Concession Area 6 (see Figure 1.1).

The following research questions are addressed:

(1) Can high-resolution imagery taken from a plane provide a more accurate estimate of kelp forest area compared to satellite imagery?

(2) What is the current biomass of the kelp forest within Concession Area 6?

(3) How does the current kelp forest map from this study area compare to those produced in previous studies?

2. Methods

2.1.Study site

The study took place along the Gansbaai coastline (Figure 2.1), which was explicitly chosen due to SAEON's provision of high-resolution imagery (HRI) for this location. The imagery was taken from a plane and captured the coastline around Danger Point Peninsula from 34° 33' 01" S, 19° 22' 03" E to 34° 36' 24" S, 19° 24' 36" E as well as Dyer Island. Within this broader region lies Concession Area 6 (Figure 2.1).

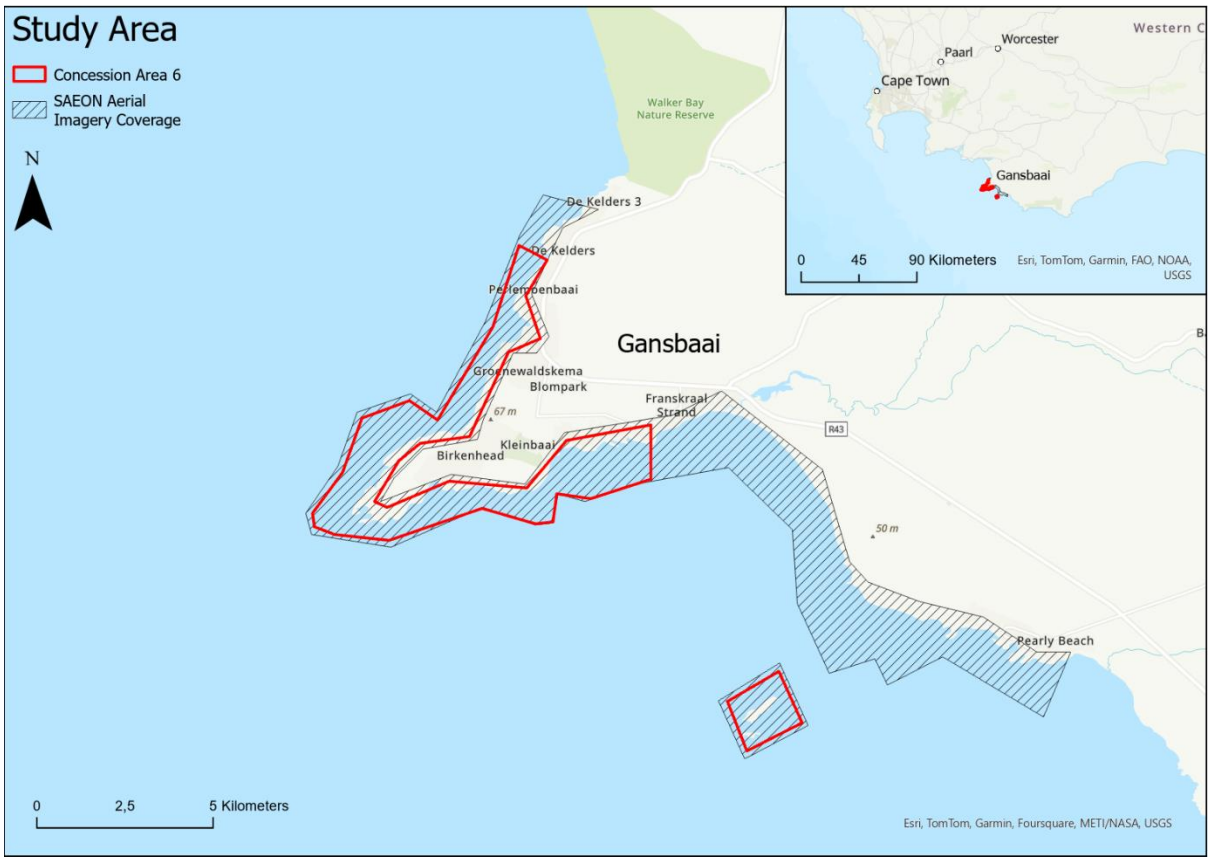

Figure 1.1. The study area indicating the area that was captured by SAEON's aerial imagery and Concession Area 6

Concession Area 6 stands as the southeasternmost harvested SRCA in South Africa (see Figure 1.1). Its biogeographical significance is highlighted by its proximity to the limits of *Ecklonia maxima* kelp forests and being the southeasternmost point for subtidal populations of *Laminaria pallida*. Concession Area 6 is situated approximately 68 km from the former easternmost *Ecklonia maxima* kelp forests. Consequently, Concession Area 6 falls within a

marine environment situated in close proximity to the limits of inshore *E. maxima* forests. This observed limit in the distribution of west coast kelp species suggests a gradient in environmental conditions within this region.

Taurus Chemicals Cape Kelp (Pty) Ltd holds the kelp harvesting rights for Concession Area 6 and harvests *Ecklonia maxima*. The Concession Area runs along the Gansbaai Coastline from the Western bank of the Uilenkraal River (34° 36' 24" S, 19° 24' 36" E to the eastern bank of the Mossel River (34° 24' 30" S, 19° 16' 24" E) and includes Dyer Island and its neighbouring reefs (Figure 2.1). To create kelp reserves within this Concession, no kelp harvesting is permitted in the following areas: From Stanford's Cove (34° 34' 06" S, 19° 21' 20" E) to Voorsteklip (34° 31' 00" S, 19° 22' 20" E; from Blousloep (34° 36' 50" S, 19° 23' 18" E) to the western bank of the Uilenkraal River; and within 500m of Dyer Island.

The term 'kelp forest' is used in this study as a singular noun to describe all of the kelp contained within the study area; the term 'kelp beds' describes discrete patches of kelp delineated by Taurus Chemicals Cape Kelp (Pty) Ltd within the larger singular kelp forest.

2.2.Procedure diagram

To answer the research questions in this study, the following processes (Figure 2.2) were followed: The S-2 satellite imagery and HRI (aerial) imagery underwent masking to remove land features. Next, the masked S-2 imagery was used to create a NDVI imagery. The masked HRI and NDVI map underwent image classification to identify kelp, water, and rocks. The classified data was then assessed for accuracy and refined and post-processed to generate a detailed kelp map. From this kelp map, the kelp canopy and total kelp biomass were calculated. Finally, the results were compared to previous studies' kelp maps, and differences were investigated to provide insights into the kelp bed characteristics and changes over time.

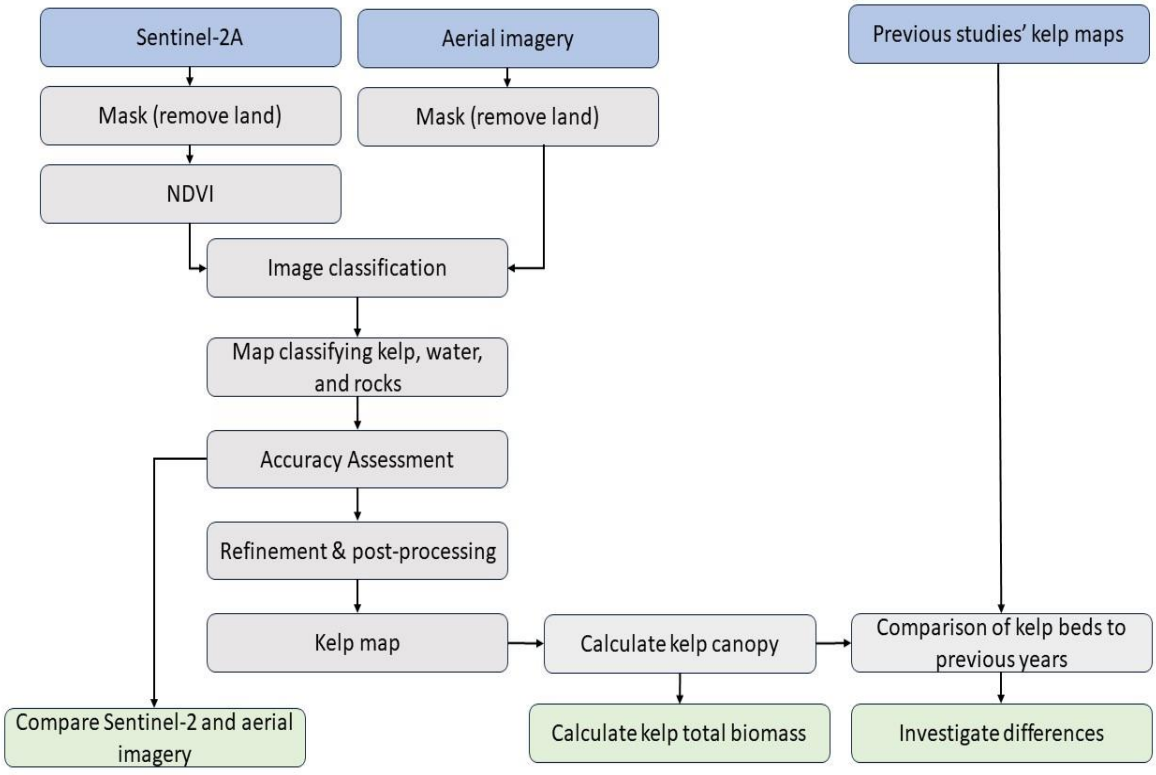

Figure 2.2. Simplified workflow of this study indicating the input data in blue, processes in grey, and the provisional outputs in green.

2.3. Input data

2.3.1. High-resolution imagery

High-resolution imagery (HRI) of the study was provided by the South African Environmental Observation Network (SAEON). The HRI was captured during low tide (0.30m above Chart Datum at 10h45) on the 6th of June 2023 from 09h44 to 12h09. The survey was done at a height of 1900ft with 100 images taken. Dyer Island was surveyed during low tide (0.37m above Chart Datum at 11h35) on the 7th of June 2023 from 11h36 to 12h18, and 142 images were taken. The equipment used for this study can be found in Table 2.1. During the survey, ground-truthing points were taken to validate the presence of kelp (see more information regarding ground-truthing in Appendix B).

Table 1.1. The equipment used by SAEON to survey the Gansbaai Coast and Dyer Island.

Equipment	Description
Aircraft	Glasair Sportsman GS2 aircraft.
Lidar	ELMAP 15V Airborne Lidar.
Camera	Nikon D850 DSLR with 24mm lens.
Global Navigation Satellite System (GNSS)	Novatel PwrPak7 SPAN (Synchronous Position, Attitude and Navigation) Receiver.
Inertial Measurement Unit (IMU)	Sensonor STIM300 IMU (Inertial Measurement Unit).

SAEON processed the imagery from the survey to produce LiDAR imagery as well as orthophotos with a pixel size of 13cm on the ground. The orthophotos produced contained artefacts such as blank spots and warping. Therefore, the LiDAR imagery provided by SAEON was used to fill in the data gaps in these areas.

To facilitate the analysis of the HRI, the orthophoto was divided into eight smaller photos because the original size (13 GB) was too large to process in a single instance. This division facilitates more manageable and efficient processing. The eight orthophotos underwent a land

masking process to remove land from the imagery and simplify the classification. This was done to specifically focus on kelp classification, as terrestrial vegetation had the potential to be confused with kelp.

2.3.2. Sentinel-2 satellite imagery

Sentinel-2A (S-2A) imagery was chosen as atmospheric corrections have already been applied; therefore, it excludes the effect of light reflected off of the earth's surface into the sensor. S-2A imagery was acquired freely from the Copernicus Browser (https://dataspace.copernicus.eu/browser), an online hub provided by the European Space Agency (ESA) for Sentinel-2 products. This browser allows users to download raw band layers from B1 to B12 (see Table 1.1).

To create an NDVI (Figure 2.3A) and a RGB map (Figure 2.3B), bands B2, B3, B4, and B8 were acquired in June 2023. Due to tidal height and cloud coverage affecting kelp visibility, days with the highest kelp visibility were prioritised. Before the supervised image classification could take place, the raw band rasters were masked to remove land. Additionally, bands B2, B3, and B4 were combined to make a RGB map (Figure 2.3B).

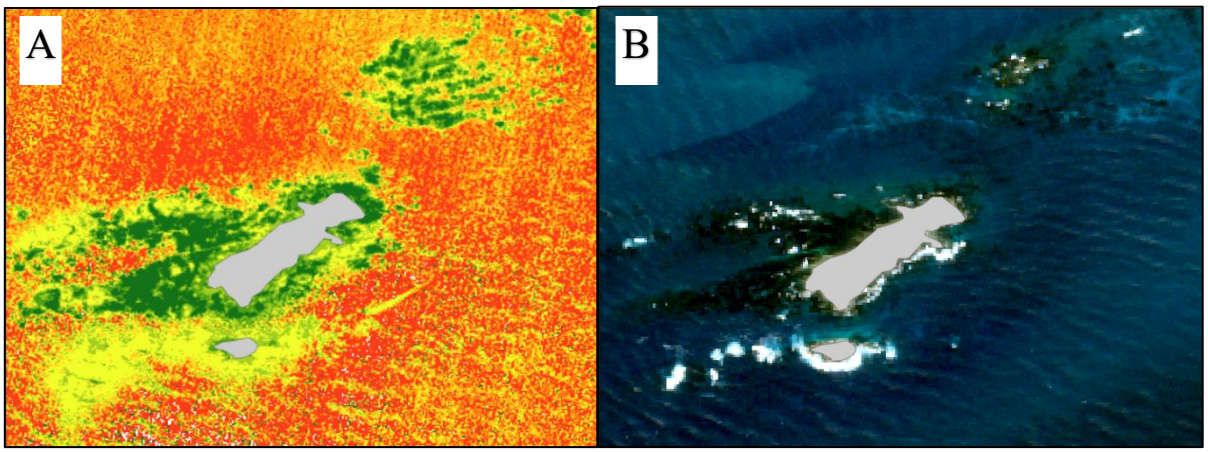

Figure 2.3. Sentinel-2 band compositions of Dyer Island shown as a NDVI map and RGB. NDVI Map (A) with vegetation shown in green and a true-colour image (RGB) (B) with kelps appearing as dark brown patches.

2.4. Normalised Difference Vegetation Index (NDVI)

The spectral bands from the S-2 imagery can be used to create NDVI maps. NDVI is a widely implemented remote-sensing metric for quantifying vegetation health and density based on the reflectance of near-infrared (NIR) and red light. NDVI is calculated using the formula:

$$NDVI = \frac{(NIR-Red)}{(NIR+Red)} \quad (1.1)$$

This formula results in values that range from -1 to 1. High positive values indicate dense vegetation, while low or negative values indicate non-vegetated surfaces such as water or rocks (Bell, Cavanaugh & Siegel, 2015; Lillesand, Kiefer & Chipman, 2015; Gendall et al., 2023). The inclusion of the NIR band is particularly crucial in mapping kelp, as it enables the discrimination between rock and kelp. Kelps, being photosynthetic organisms, contain chlorophyll which predominately absorbs light in the visible spectrum and absorbs less in the NIR range. Consequently, they have a high reflectance in the NIR range. By analysing the NDVI values derived from satellite imagery, researchers can effectively distinguish kelp from water and rocks, therefore allowing for the extent of kelp forests to be mapped (Rand, 2006; Uhl, Bartsch & Oppelt, 2016).

Using a raster calculator tool in ArcGIS Pro 3.1.0 (Esri, 2023), the NDVI equation was applied to bands B4 and B8 to produce an NDVI map (Figure 2.3). The NIR and red bands capture distinct spectral properties of water, rock, and kelp. Leveraging these differences, NDVI thresholds can be derived. These thresholds facilitate the effective separation of kelp from water and rocks, allowing for the classification of these elements. The spectral values corresponding to these classes were extracted from the NDVI map for supervised image classification.

2.5. Supervised image classification

Supervised image classification is the process in which a computer algorithm is trained to categorise digital images into predefined classes (Sibaruddin et al., 2018). The algorithm learns to identify patterns and features within the training data that are indicative of the different classes, and it uses this knowledge to make predictions about the classes within the study area (Lillesand, Kiefer & Chipman, 2015; St-Pierre & Gagnon, 2020). Pixel classification, the method used in this study, is an image-processing technique used to categorise individual pixels in an image into predefined classes or categories. This method was chosen as it is commonly used in kelp bed mapping studies (Bennion et al., 2019)

Supervised Maximum Likelihood Classification (MLC) of the HRI and the NDVI map was done using ArcGIS Pro 3.1.0. In the process of MLC, the likelihood of pixels being associated with each of the trained classes is computed (Lillesand, Kiefer & Chipman, 2015). For the MLC, training polygons were created based on ground-truthing points taken during the SAEON survey and areas where kelp could be clearly visualised in the HRI. These training polygons were used to categorise the pixels within the imagery into three classes, namely class 1 (kelp), class 2 (water), and class 3 (rock/land). The output of this process was a classified raster indicating areas of kelp, water, and rock/land. The output rasters were converted shapefiles containing polygons for better visualisation and accurate calculations of geometric attributes such as area.

2.6. Accuracy assessment

To investigate and compare the accuracy of the supervised image classification of the S-2A imagery to the high-resolution imagery, both a visual assessment and confusion matrix were conducted.

2.6.1 Visual assessment

The visual validation process entailed panning the entire extent covered by the new kelp polygons map to check for areas incorrectly classified. The ground-truthing points were also compared to the classified rasters to further verify the classification.

2.6.2 Confusion matrix

A confusion matrix was constructed in ArcGIS Pro 3.1.0 using accuracy assessment points. Accuracy assessment points are used to evaluate the performance of a supervised image classification algorithm by comparing the class assigned by the algorithm to known reference data. For this study, the classes assigned were compared to the HRI as the resolution was sufficiently high to provide clear visibility and a detailed depiction of the contents within the image. These assessment points were used to create a confusion matrix computing the User's Accuracy, Producer's Accuracy, overall accuracy and kappa coefficient. This matrix provides a clear and quantitative representation of the supervised classification algorithm's performance, highlighting areas of strength and improvement.

2.7. Post-processing

To improve the accuracy of the kelp maps before proceeding with biomass estimations and comparisons to previous studies, the maps were cleaned by manually removing areas incorrectly classified as kelp. Additionally, the high-resolution imagery contained some artefacts such as distortions and blank regions that arose during the orthorectification of the imagery. To overcome this, in areas in which kelp was distorted and classified incorrectly, the features were removed and reclassified manually using the LiDAR imagery.

2.8. Current kelp biomass estimation

Once the kelp within the study area was mapped from the high-resolution imagery, the overall area of the kelp forest (m^2) was calculated. The second piece of information required to

calculate the total biomass of the kelp forest is an average kelp biomass figure (per m^2). Currently, the only available kelp biomass figure that is applicable to Concession Area 6 is that determined in Rothman (2006). Rothman (2006) calculated an average *Ecklonia maxima* biomass figure (per m^2) for the Cape Peninsula and West Coast of South Africa. This was achieved by cutting and weighing kelp from $1m^2$ quadrats.

Using this figure of 14.5 ± 1.33 kg/m^2 (Rothman, 2006), the overall biomass of the study area could be calculated using this equation, also from Rothman (2006):

$$b = w \times a, \qquad (2.1)$$

where b is the biomass of the entire study area, w is the average biomass per m^2 (kg/m^2), and a is the area of the kelp bed (m^2). It must be noted that this is an average kelp biomass measurement. The biomass measurements by Rothman (2006) varied between study sites with the lowest biomass figure of 10 kg/m^2 at shallower sites and the highest biomass 21.3 kg/m^2 at deeper sites.

2.9 Comparison of current kelp area to previous years

elp forest calculated in this study was compared to those made in previous studies (Table 2.2). Shapefiles of the kelp forest created by (Rand, 2006) and published in Anderson et al. (2007) were provided. Additionally, shapefiles were provided from Dunga (2019) and Taurus Chemicals Cape Kelp (Pty) Ltd. The data used by Anderson et al. (2007) covers Concession Area 6 but excludes Dyer Island. Consequently, changes in kelp extent were only compared around Danger Point Peninsula (see Figure 2.4).

Table 2.2 The input data used to investigate the changes in kelp extent and kelp beds within Concession Area 6 with tidal heights referenced to Mean Lower Low Water (MLLW). Pixel resolution refers to the Ground Sampling Distance at the equator.

Input Mapping Data	Description	Dates of acquisition	Pixel resolution	Tidal Height
Anderson et al. (2007)	Digitised Tarr (1993) Infrared maps	1993	2m	0.13m
Dunga (2019)	Sentinel L2C Satellite data	2016	20m	1.74m
This study	Sentinel L2A Satellite data	2023	20m	0.6m
This study	High-resolution imagery	2023	13cm	0.30 (Coastline) 0.37 (Dyer Island)

3. Results

3.1. Supervised image classification

The supervised image classification resulted in maps indicating the area and extent of kelp around Danger Point Peninsula and Dyer Island. The output polygons of the HRI are much more detailed than the polygons created from the S-2A imagery (Figure 3.1).

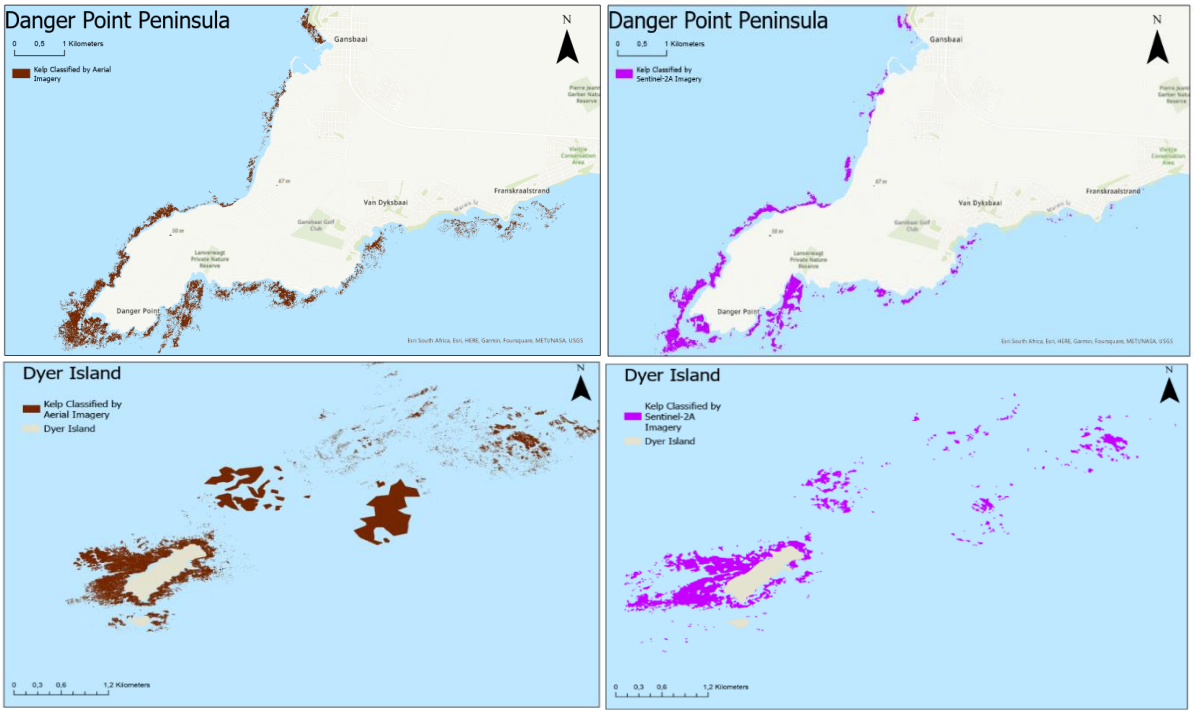

Figure 3.1. Maps showing the area classified by the supervised image classification as kelp around Danger Point (Top) and Dyer Island (bottom). The output kelp polygons of the of the S-2A imagery can be viewed on the right and the output of the HRI on the left.

3.2 Accuracy assessment

To assess the accuracy of the MLC in Figure 3.1, confusion matrices were produced for the output of the S-2A imagery as well as the HRI. Table 3.1 shows the results of the accuracy assessment of the kelp classification using high-resolution imagery as input. The matrix shows that 45 of the 50 validation points for kelp were classified correctly as kelp (90%). All 50 validation points of water were classified correctly, and of the 50 validation points for rock, 47 points were classified correctly (94%). This led to an overall producers' accuracy (Type 1 error) of 94% and a general users' accuracy (Type 2 error) of 95%. The overall accuracy is 95%. The kappa coefficient, which provides a comprehensive evaluation of the accuracy of the classification, is very high (0.92 from a possible range of -1 (no agreement) to 1 (full agreement).

Table 2.1 Confusion matrix for the supervised image classification of the HRI of the Gansbaai Coastline.

Class	Kelp	Water	Rock	Total
Kelp	45	3	2	50
Water	0	50	0	50
Rock	3	0	47	50
Total	48	53	49	150
Producer's Accuracy (%)	0,93	0,94	0,95	**0,94**
User's Accuracy (%)	0,9	1	0,94	**0,95**
Overall accuracy (%)				**0,95**
Kappa statistics				**0,92**

Table 3.2 shows the results of the accuracy assessment of the MLC using the S-2A imagery as input. The matrix shows that 36 of the 50 validation points for kelp were classified correctly as kelp (72%). Of the 50 validation points for water, 49 were classified correctly (98%), and of the 50 validation points for rock, 27 points were classified correctly (54%). This leads to an overall producers' accuracy (Type 1 error) of 79% and an overall users' accuracy (Type 2 error) of 76%. This results in an overall accuracy of 75%. The kappa coefficient still substantial (0.62 from a possible range of -1 (no agreement) to 1 (full agreement)).

Table 3.2 Confusion matrix for the supervised image classification of Sentinel-2A imagery.

Class	Kelp	Water	Rock	Total
Kelp	36	12	2	50
Water	1	49	0	50
Rock	8	15	27	50
Total	45	76	29	150
Producer's Accuracy	0,80	0,65	0,93	**0,79**
User's Accuracy	0,72	0,98	0,54	**0,76**
Overall accuracy (%)				**75**
Kappa statistics				**0,62**

The overall accuracy and kappa coefficient of the HRI's classification was greater than that of the S-2A satellite data. The visual comparisons (Figure 3.2) provide additional support to these findings, as they revealed instances where the classification failed to identify certain areas of kelp. for example, water gullies between the kelp were erroneously classified as kelp, and areas sparse in kelp were often not identified. Additionally, the S-2A imagery had more cases in which rocks were incorrectly classified as kelp (Table 3.2).

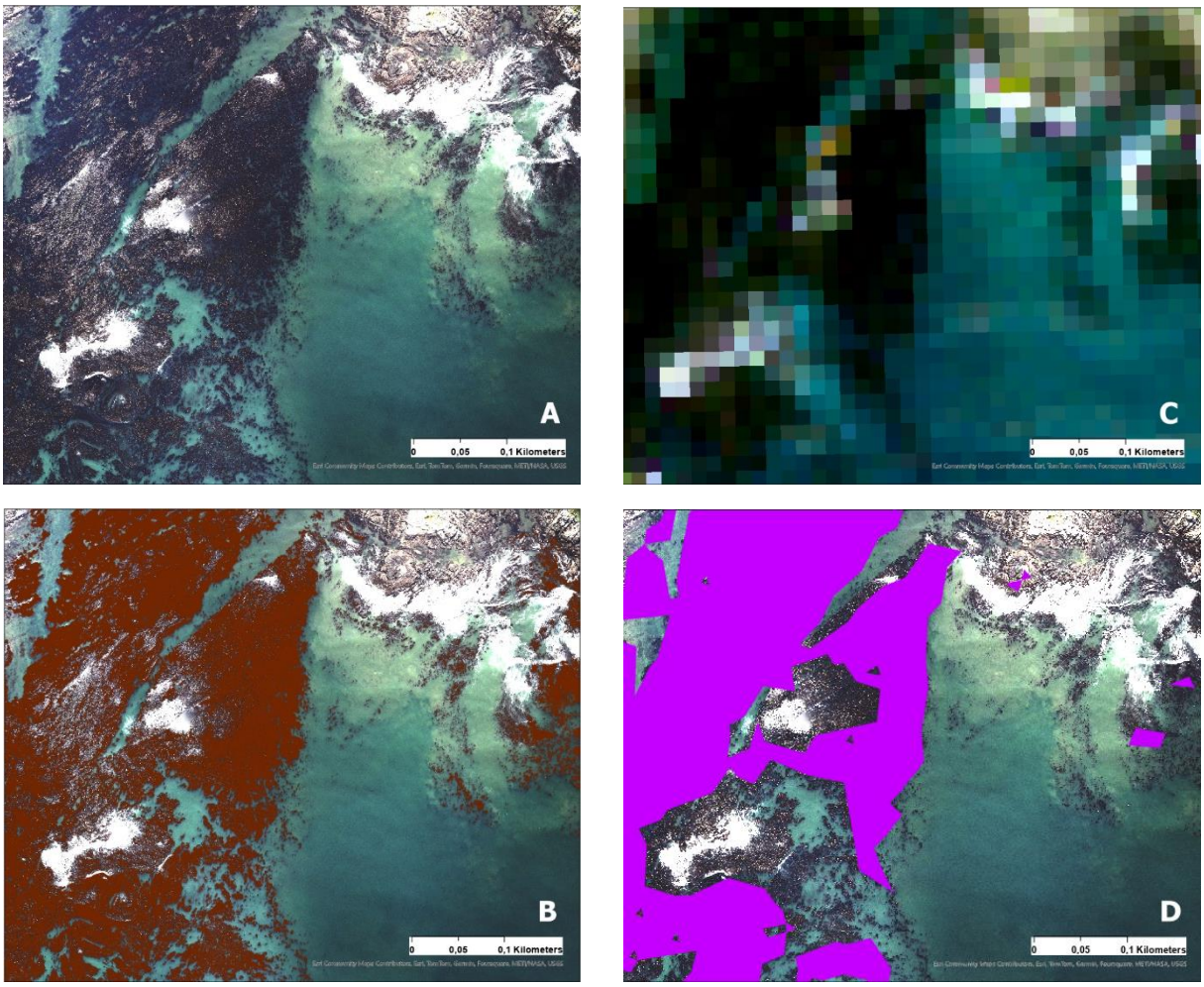

Figure 2.2. Comparison of the raw HRI (A) to the raw S-2A imagery(C). Comparison of the kelp polygons produced from HRI (B) and S-2A imagery (D) overlayed onto the raw HRI.

3.3. Kelp biomass estimation

The coupling of HRI and MLC produced a highly accurate kelp forest map. Consequently, this map was used to calculate the kelp forest area and biomass (Table 3.3).

Table 3.3. The total area and biomass of kelp within Concession Area 6. This was calculated using the product of the area of kelp (determined from the HRI) and Rothman's kelp biomass figure with standard error (2006), see section 2.8.

Area of Interest	Area of kelp (m^2)	Biomass kelp (tonnes)
Concession Area 6	2 795 025.3	40527.9 ± 3717.4

3.4. Comparison of this study to previous studies

The kelp area measurements of this study and previous studies (see Table 2.2) around Danger Point indicate that the maps of previous studies estimated the extent of kelp to be greater by a maximum of 161.27% compared to the kelp estimations done using HRI (Figure 3.4). The kelp extent in 1993 produced from Anderson et al. (2007) data estimated the greatest kelp extent, whereas the kelp extent produced from the high-resolution imagery had the smallest estimate. The difference between the 1993 kelp map by Anderson et al. (2007) and the 2023 HRI is 263.94ha (a difference of 61.71%).

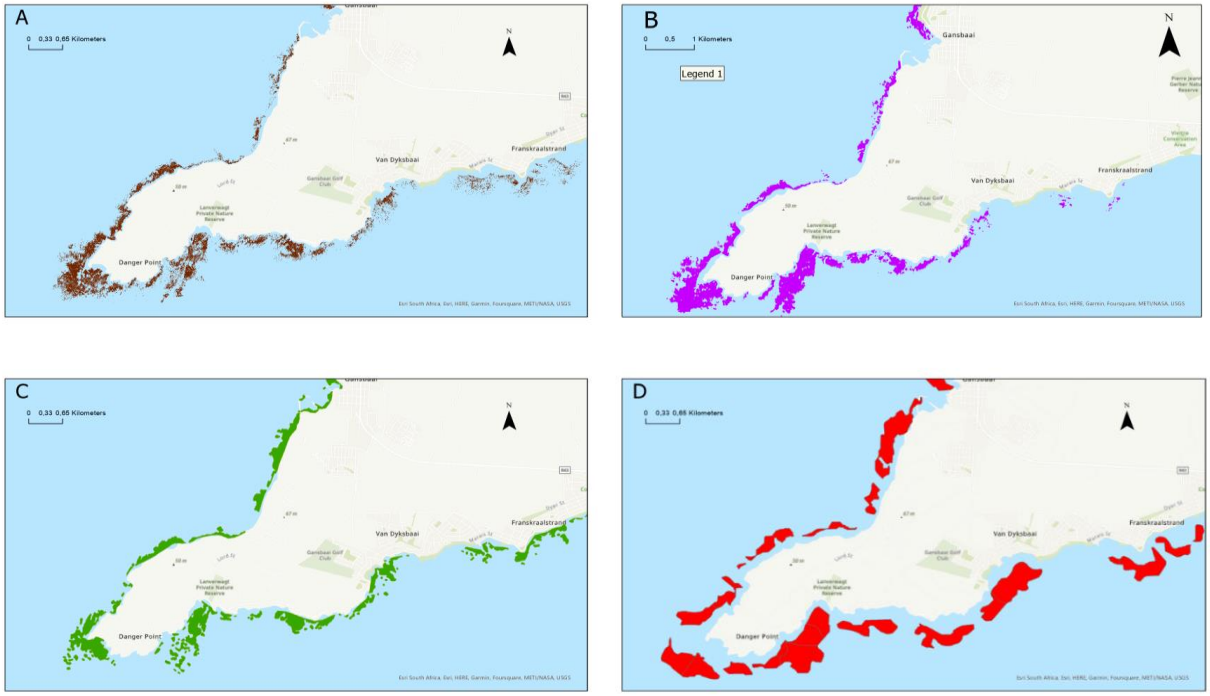

Figure 3.3. The kelp forests maps of Danger Point Peninsula. (A) Kelp extent mapped from high-resolution imagery, (B) kelp extent mapped from S-2A 2023 imagery, (C) Kelp extent mapped by Dunga (2019) and (D) kelp extent mapped by Anderson et al. (2007).

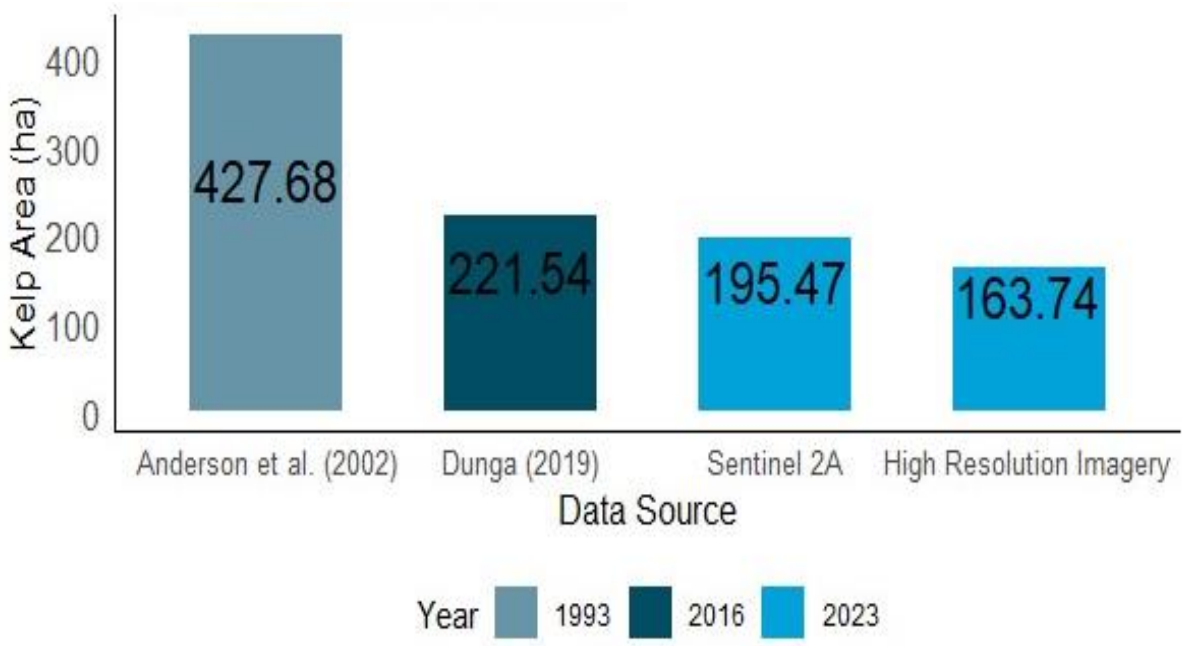

Figure 3.4. The extent of kelp area (ha) around Danger Point Peninsula of current and past studies.

Visual comparisons of the kelp maps indicate that the classification of the HRI performed better in delineating the extent of the kelp forest around Danger Point Peninsula (Figure 3.6; see more in Appendix C). The classification of S-2A showed many instances where rock and water were incorrectly classified as kelp. The kelp extent mapped by Anderson et al. (2007) indicated many instances of kelp where it was not actually present while simultaneously overlooking significant kelp beds. The maps made by Dunga (2019) also failed to identify some areas of kelp accurately, and mistakenly classified some sections of rock as kelp.

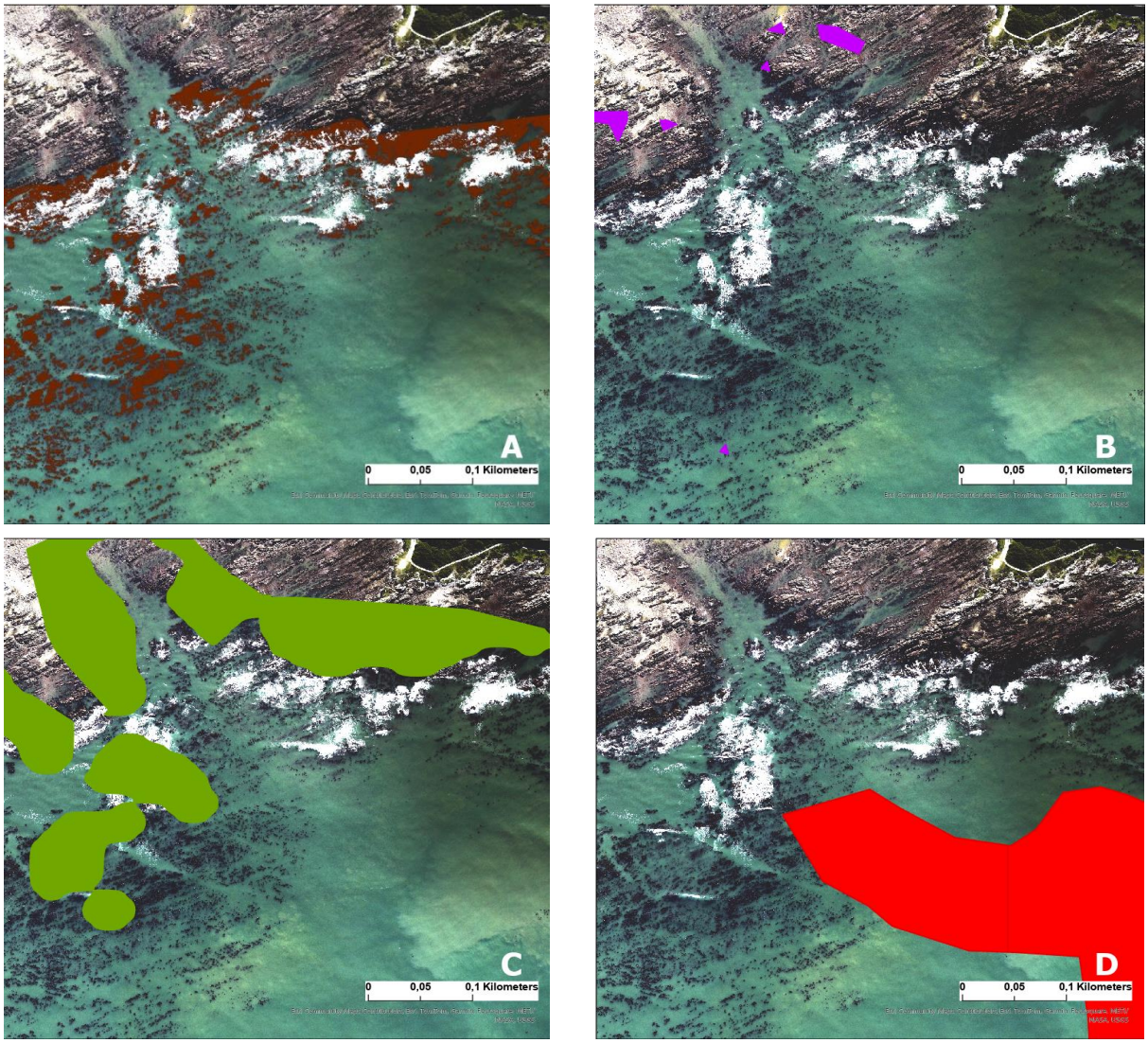

Figure 3.6. A zoomed in comparison of the kelp maps. With the kelp extent mapped from the high-resolution imagery (A). S2-A kelp extent from this study (B), Dunga (2019) kelp extent (C) and Anderson et al. (2007) kelp extent (D).

4. Discussion

4.1. Comparative accuracy of high-resolution imagery versus Sentinel-2 satellite imagery.

With advances in remote sensing technology, opportunities to map and monitor important seascapes over large extents are increasing (Gendall et al., 2023). This study has shown that HRI offers a great tool to map kelp forests in South African SRCAs.

The confusion matrix for the S-2A classification indicated a relatively high producer's accuracy for kelp classification (0.8), demonstrating that when the classifier predicted instances of kelp it was frequently correct (Table 3.2). However, the user's accuracy suggests that it did not capture all actual instances of kelp. This discrepancy is likely due to false positives where instances of water or rock were incorrectly classified as kelp (as seen in Figure 3.6). These false positives contribute to an overestimation of kelp area and an inaccurate map of the extent of kelp.

The high user and producer accuracy measures of the HRI classification indicate that the model is effective in distinguishing between kelp, rock, and water. Consequently, the use of HRI results in a robust classifier, ensuring reliable estimation of kelp extent. These results are similar to several studies which found that higher resolution imagery resulted in higher confidence in kelp detection (Berry & Crowdrey, 2021; Cavanaugh, Bell, et al., 2021; Cavanaugh, Cavanaugh, et al., 2021; Chen et al., 2022).

There are several reasons why the high-resolution imagery contributes to a more accurate classification. First, it provides finer details allowing the classifier to make more precise distinctions between the classes (Bennion et al., 2019). For instance, it can capture fine-scale landscape characteristics such as water gullies within the kelp forest. Second, the colour variations between the classes are better distinguished, enabling the classification algorithm to make more refined decisions. Third, higher-resolution imagery reduces the occurrence of

mixed pixels, where a single pixel contains a combination of different classes (more common in lower-resolution imagery). The reduction in mixed pixels makes it easier for the classifier to assign accurate labels to the individual pixels (Lillesand, Kiefer & Chipman, 2015; Schroeder et al., 2019).

In contrast, the lower resolution of satellite imagery has been demonstrated to produce less accurate kelp maps (Deysher, 1993; Stekoll, Deysher & Hess, 2006). A study done in California by Deysher (1993) shows that SPOT satellite imagery (20m resolution) is insufficient for smaller beds in this region. Additionally, Stekoll et al. (2006) found that Landsat 7 satellite imagery (15m resolution) overestimated the area of the kelp canopy of *Nereocystis luetkeana*, a kelp with a morphology similar to that of *E. maxima*. The overestimation of kelp extent, due to a lower resolution, indicates that S-2A imagery is insufficient to create highly accurate maps, such as those needed for biomass estimates of Concession Areas.

Although high-resolution imagery can yield a very accurate kelp map, employing it to assess kelp coverage across an extensive area would be impractical due to the expenses associated with flying a plane over such large regions. Studies conducted over larger extents, which do not aim to calculate MSY, do not require high levels of accuracy. Therefore, freely available satellite imagery, such as Sentinel-2 imagery, with its broader coverage is a more practical option for producing kelp distribution maps. Although it doesn't produce extremely accurate kelp maps, Sentinel-2 imagery proved ideal in Dunga (2019), which aimed at mapping kelp for conservation purposes, focusing on identifying the locations of kelp forests rather than determining biomass.

4.2. Comparison of kelp forest maps around Danger Point Peninsula

The comparison of kelp maps around Danger Point Peninsula reveals notable discrepancies in kelp extent estimates among the studies. The findings suggest that earlier studies had a greater

kelp extent compared to the high-resolution imagery used in the current investigation. As the classification of the high-resolution imagery has shown to be very accurate, this divergence prompts questions about the accuracy and reliability of methodologies employed in earlier studies. The difference of 263.94ha in kelp extent between the 1993 map by Anderson et al. (2007) and the 2023 HRI highlights this point.

The visual analysis of the kelp maps highlighted many instances where the previous studies misclassified water and rock as kelp. The misclassifications observed in the S-2A imagery (2023) and in Dunga (2019) are likely due to the low pixel resolution. In Figure 3.4, it is evident that Anderson et al. (2007) classified areas of kelp that are not visible in the high-resolution imagery. This inconsistency may be attributed to the lower tides, which was 17cm lower during image acquisition in Anderson et al. (2007). Additionally, Anderson et al. (2007) used Infrared maps from Tarr (1993) which had a lower resolution and a limited spectral resolution, making it challenging to accurately distinguish kelp from other features or environmental conditions (Lillesand, Kiefer & Chipman, 2015).

It is evident that the difference in measured kelp extent from 1993 to 2023 (Figure 3.3) is likely not the result of overharvesting. Rather, it is the result of recent shifts toward more accurate methods of measurement that are less likely to overestimate kelp extent. Further supporting this is the decrease in the measured extent of non-harvested kelp beds from 1993 to 2023. Accurate conclusions about the impact of harvesting cannot be made using measurements drawn from imagery of varying quality (for example, high resolution compared to lower resolution).

Drawing conclusions about the differences between kelp maps becomes challenging when considering variations in tidal height during imagery capture across different studies (see Table 3). Specifically, a lower tide reveals more *E. maxima* heads, making them more visible; this is

due to the gas-filled bulbs at the top of the stipe suspending the fronds near the sea surface (Rothman et al., 2010). Consequently, higher tides, as observed in the satellite image capture during Dunga (2019), may substantially diminish the visible extent of kelp forests. This limitation underscores another drawback of utilizing satellite imagery for continuous monitoring of kelp forests in Concession Areas, as aligning image capture with low tidal heights is difficult (Cavanaugh, Bell, et al., 2021).

The results underscore the value of utilising HRI for accurate and reliable kelp mapping, as it provides finer details crucial for accurate estimations and can be planned to coincide with low spring tides as done in this study. Inaccuracies in mapping could have ecological implications, as misidentifying kelp beds or neglecting their presence may impact ecosystem assessments and conservation efforts. Furthermore, accurate biomass estimates are crucial for enhancing the quality of MSY assessments, thus providing a reliable basis for optimizing sustainable harvesting practices.

4.3. Limitations and Recommendations

One limitation of this study is the utilization of an average kelp biomass figure for the Cape Peninsula and West coast to estimate the total biomass of Concession Area 6. Kelp biomass estimates have shown to significantly vary between sites (Rothman, 2006; Anderson et al., 2007).While using an average figure of 14.5 kg/m^2 provides a baseline, it may fail to consider the changes in kelp biomass in deeper or more dense sites in Concession Area 6 and result in an overestimation or underestimation of the total biomass. To enhance the accuracy of the total kelp biomass estimation, it is recommended that kelp biomass measurements be conducted within the Concession Area of interest prior to mapping (Table 3). Additionally, these biomass estimates should account for depth and density variations. *Ecklonia maxima* has been observed to decrease in density with an increase in depth (Rothman, 2006). In deeper waters, kelp exhibits longer, heavier stipes with greater frond biomass compared to shallower kelp.

To support accurate MSY measurements, it is advisable to employ a framework that considers these variables. The recommendations for future kelp biomass estimates in South African Concession Areas include: establishing a biomass estimation specific to the Concession Area, developing quality criteria for image capture (e.g. tidal heights, sun angles, and sensor specifications), using pixel-based image classification to identify kelp, collecting in-situ ground-truthing data for accuracy assessment, and utilizing high-resolution imagery for more accurate kelp extent measurements and biomass estimations (see Table 3).

Table 3. Recommendations for future kelp biomass estimates in South African Concession Areas.

Parameters	Concession Area kelp biomass estimation framework recommendations
Biomass estimation figure	Should be done in Concession Area of interest prior to image capture. Data such as bathymetry and kelp bed density should be taken into consideration for biomass estimations.
Quality Criteria for image capture	Have a set of quality criteria for adapted for the specific Concession Area. Things to consider in the development of the criteria: Aim for spring low tidal heights; Minimise low sun angles and shadows; Minimise haze and cloud cover. Include NIR or red-edge wave band when selecting the sensor to assist with distinguishing between rock and kelp and reduce potential of overestimation.
Classification	To classify kelp, use a pixel-based image classification.
Accuracy Assessment	In situ, ground-truthing data should be collected on the day of each survey. Where this is not possible, other data can be used to validate the classification such as expert knowledge, and past surveys which show the location of the kelp forests.
Resolution	High-resolution (<1m) is recommended when estimating the kelp biomass for a maximum sustainable yield. A higher resolution results in more accurate kelp extent measurements, ultimately allowing for a more accurate biomass estimation

The potential influence of climate change on total kelp biomass cannot be definitively ruled out, even though there is currently no evidence to support this assertion. Considering

Concession Area 6's proximity to the limits of *Ecklonia maxima* distribution and that *E. maxima*'s distribution range is hypothesised to be defined by water temperatures limits (Bolton et al., 2012; Rothman et al., 2017), it is strongly recommended that continuous monitoring of kelp populations be conducted, accompanied by regular temperature measurements.

Conclusions

It is apparent that over the last 20 years, harvesting in Concession Area 6 was conducted based on an overestimation of the inshore kelp standing stock. However, monitoring by the DFFE indicated that these harvesting practices had a negligible impact on the resource, affirming the sustainability of harvesting at the current MSY (DFFE, 2024; Dr Mark Rothman, pers. comm). Two potential explanations for this finding are considered: first, the average biomass figure used for calculating the standing stock may be too low for the area; second, the conservative notion that only 10% of the standing stock can be harvested may be overly cautious. However, it is crucial to recognize the variability in kelp forest density at different sites, emphasizing the need for a site-specific assessment.

This study highlights the potential role of HRI in accurately mapping and monitoring kelp forests in South African Concession Areas. The limitations of S-2A imagery, particularly its lower resolution and susceptibility to misclassifications, were evident in the study, emphasizing its inadequacy for mapping an accurate kelp extent needed for MSY. While HRI delivers accurate results, its feasibility diminishes over extremely large areas, making S-2 satellite imagery a more practical option for broader coverage studies. The comparison of kelp forest maps around Danger Point Peninsula revealed substantial discrepancies between earlier studies and the high-resolution imagery used in this investigation. The overestimation in earlier studies raises questions about the accuracy of methodologies employed, further emphasizing the need for reliable and comparable mapping techniques.

It is essential to acknowledge that different species of kelp may require slightly different methods. While the methods in this study have proven successful for *Ecklonia maxima*, they may not be applicable to *Macrocystis pyrifera* which has continuous canopy of fronds forming a surface canopy. In summary, the utilization of HRI emerges as an excellent tool for accurate kelp mapping, with profound implications for ecological assessments and conservation efforts. The study contributes valuable insights and recommendations, emphasizing the need for methodological consistency and site-specific considerations in future kelp monitoring and biomass estimation endeavours. In the context of South Africa Concession Areas, where accurate kelp canopy classification is fundamental, the use of higher-resolution imagery becomes especially important. Accurate classification not only ensures a comprehensive understanding of the landscape but also facilitates better estimations of maximum sustainable yields, thereby allowing for more effective resource management.

Reference list:

Al-doski, J., Mansor, S.B., Zulhaidi, H. & Shafri, M. 2013. Image Classification in Remote Sensing. *Journal of Environment and Earth Science*. 3(10):141–148.

Anderson, R.J., Rothman, M.D., Share, A. & Drummond, H. 2006. Harvesting of the kelp Ecklonia maxima in South Africa affects its three obligate, red algal epiphytes. *Journal of Applied Phycology*. 18(3–5):343–349. DOI: 10.1007/s10811-006-9037-7.

Anderson, R.J., Rand, A., Rothman, M.D., Share, A. & Bolton, J.J. 2007. Mapping and quantifying the South African kelp resource. *African Journal of Marine Science*. 29(3):369–378. DOI: 10.2989/AJMS.2007.29.3.5.335.

Bell, T.W., Cavanaugh, K.C. & Siegel, D.A. 2015. Remote monitoring of giant kelp biomass and physiological condition: An evaluation of the potential for the Hyperspectral Infrared Imager (HyspIRI) mission. *Remote Sensing of Environment*. 167:218–228. DOI: 10.1016/j.rse.2015.05.003.

Bennion, M., Fisher, J., Yesson, C. & Brodie, J. 2019. Remote sensing of kelp (Laminariales, Ochrophyta): monitoring tools and implications for wild harvesting. *Reviews in Fisheries Science and Aquaculture*. 27(2):127–141. DOI: 10.1134/s0320972519100129.

Berry, H. & Crowdrey, T. 2021. Kelp Forest Canopy Surveys with Unmanned Aerial Vehicles (UAVs) and Fixed-Wing Aircraft: A demonstation Project at Volunteer Monitoring Sites in Northern Pudget Sound. Available: https://www.dnr.wa.gov/publications/aqr_nrsh_kelp_canopy_survey_report.pdf.

Blamey, L.K. & Bolton, J.J. 2018. The economic value of South African kelp forests and temperate reefs: Past, present and future. *Journal of Marine Systems*. 188:172–181. DOI: 10.1016/j.jmarsys.2017.06.003.

Bolton, J. 2016. What is aquatic botany?- And why algae are plants: The importance of non-taxonomic terms for groups of organisms. *Aquatic Botany*. 132. DOI: 10.1016/j.aquabot.2016.02.006.

Bolton, J.J. 2010. The biogeography of kelps (Laminariales, Phaeophyceae): A global analysis with new insights from recent advances in molecular phylogenetics. *Helgoland Marine Research*. 64(4):263–279. DOI: 10.1007/s10152-010-0211-6.

Bolton, J.J., Anderson, R.J., Smit, A.J. & Rothman, M.D. 2012. South African Kelp Moving Eastwards: The Discovery of Ecklonia Maxima (Osbeck) Papenfuss at De Hoop Nature Reserve on the South Coast of South Africa. *African Journal of Marine Science*. 34(1):147–151. DOI: 10.2989/1814232X.2012.675125.

BSASA. 2023. *Kelp value chain analysis, market assessment and roadmap for development of kelp farming in South Africa*.

Cavanaugh, K.C., Cavanaugh, K.C., Bell, T.W. & Hockridge, E.G. 2021. An Automated Method for Mapping Giant Kelp Canopy Dynamics from UAV. *Frontiers in Environmental Science*. 8(February):1–16. DOI: 10.3389/fenvs.2020.587354.

Cavanaugh, K.C., Bell, T., Costa, M., Eddy, N.E., Gendall, L., Gleason, M.G., Hessing-Lewis, M., Martone, R., et al. 2021. A Review of the Opportunities and Challenges for Using Remote Sensing for Management of Surface-Canopy Forming Kelps. *Frontiers in Marine Science*. 8(October). DOI: 10.3389/fmars.2021.753531.

Chen, J., Li, X., Wang, K., Zhang, S., Li, J. & Sun, M. 2022. Assessment of intertidal seaweed biomass based on RGB imagery. *PLOS ONE*. 17(2):1–13. DOI: 10.1371/journal.pone.0263416.

Deysher, L.E. 1993. Evaluation of remote sensing techniques for monitoring giant kelp

populations. *Hydrobiologia*. 260(1):307–312. DOI: 10.1007/BF00049033.

Dunga, L.V. 2019. Mapping and assessing ecosystem threat status of South African kelp forests. University of Cape Town.

Elston, C., Anderson, R.J. & Price, L.M. 2015. Bald kelp: natural and harvesting-induced frond loss in the South African kelp Ecklonia maxima. *African Journal of Marine Science*. 37(3):373–381. DOI: 10.2989/1814232X.2015.1079555.

Esri. 2023.

Field, J.G., Griffiths, C.L., Griffiths, R.J., Jarman, N., Zoutendyk, P., Velimirov, B. & Bowes, A. 1980. Variation in structure and biomass of kelp communities along the south-west cape coast. *Transactions of the Royal Society of South Africa*. 44(2):145–203. DOI: 10.1080/00359198009520561.

Filbee-Dexter, K. & Wernberg, T. 2018. Rise of Turfs: A New Battlefront for Globally Declining Kelp Forests. *BioScience*. 68(2):64–76. DOI: 10.1093/biosci/bix147.

Gendall, L., Schroeder, S.B., Wills, P., Hessing-Lewis, M. & Costa, M. 2023. A Multi-Satellite Mapping Framework for Floating Kelp Forests. *Remote Sensing*. 15(5). DOI: 10.3390/rs15051276.

Kosek, K. & Kukliński, P. 2023. Impact of kelp forest on seawater chemistry – A review. *Marine Pollution Bulletin*. 196(July). DOI: 10.1016/j.marpolbul.2023.115655.

Levitt, G.J., Anderson, R.J., Boothroyd, C.J.T. & Kemp, F.A. 2002. The effects of kelp harvesting on its regrowth and the understorey benthic community at Danger Point, South Africa, and a new method of harvesting kelp fronds. *South African Journal of Marine Science*. 7615(24):71–85. DOI: 10.2989/025776102784528501.

Lillesand, T.M., Kiefer, R.W. & Chipman, J.W. 2015. *Remote Sensing and Image*

Interpretation.

Miller, R.J., Lafferty, K.D., Lamy, T., Kui, L., Rassweiler, A. & Reed, D.C. 2018. Giant kelp, Macrocystis pyrifera, increases faunal diversity through physical engineering. *Proceedings of the Royal Society B: Biological Sciences*. 285(1874). DOI: 10.1098/rspb.2017.2571.

Mishra, D.R. & Gould, R.W. 2016. Remote sensing in coastal environments. *Remote Sensing*. 8(8):1–6. DOI: 10.3390/rs8080665.

Murfitt, S.L., Allan, B.M., Bellgrove, A., Rattray, A., Young, M.A. & Ierodiaconou, D. 2017. Applications of unmanned aerial vehicles in intertidal reef monitoring. *Scientific Reports*. 7(1):1–11. DOI: 10.1038/s41598-017-10818-9.

Nahirnick, N.K., Reshitnyk, L., Campbell, M., Hessing-Lewis, M., Costa, M., Yakimishyn, J. & Lee, L. 2019. Mapping with confidence; delineating seagrass habitats using Unoccupied Aerial Systems (UAS). *Remote Sensing in Ecology and Conservation*. 5(2):121–135. DOI: 10.1002/rse2.98.

Nijland, W., Reshitnyk, L. & Rubidge, E. 2019. Satellite remote sensing of canopy-forming kelp on a complex coastline: A novel procedure using the Landsat image archive. *Remote Sensing of Environment*. 220(October 2018):41–50. DOI: 10.1016/j.rse.2018.10.032.

Rand, A. 2006. Using Geographic Information Systems and Remote Sensing to Improve the Management of Kelp Resources in South Africa. University of Cape Town.

Rothman, M.D. 2006. Investigations into the harvesting ecology of the South African kelp Ecklonia maxima (Alariaceae , Laminariales). University of Cape Town.

Rothman, M.D., Anderson, R.J., Bolton, J.J., Boothroyd, C.J.T. & Kemp, F. 2010. A simple method for rapid estimation of Ecklonia maxima and Laminaria pallida biomass using floating surface quadrats. *African Journal of Marine Science*. 32(1):137–143. DOI:

10.2989/18142321003714906.

Rothman, M.D., Mattio, L., Wernberg, T. & Anderson, R.J. 2015. A molecular investigation of the genus Ecklonia (Phaeophyceae, Laminariales) with special focus on the Southern Hemisphere. *Journal of phycology*. 51(2):236–246. DOI: 10.1111/jpy.12264-14-136.

Rothman, M.D., Mattio, L., Anderson, R.J. & Bolton, J.J. 2017. A phylogeographic investigation of the kelp genus Laminaria (Laminariales, Phaeophyceae), with emphasis on the South Atlantic Ocean. *Journal of Phycology*. 53(4):778–789. DOI: 10.1111/jpy.12544.

Rothman, M.D., Anderson, R.J., Kandjengo, L. & Bolton, J.J. 2020. Trends in seaweed resource use and aquaculture in South Africa and Namibia over the last 30 years. *Botanica Marina*. 63(4):315–325. DOI: 10.1515/bot-2019-0074.

Sagawa, T., Mikami, A., Aoki, M.N. & Komatsu, T. 2012. Mapping seaweed forests with IKONOS image based on bottom surface reflectance. *Remote Sensing of the Marine Environment II*. 8525(22255010):85250Q. DOI: 10.1117/12.975678.

Schroeder, S.B., Dupont, C., Boyer, L., Juanes, F. & Costa, M. 2019. Passive remote sensing technology for mapping bull kelp (Nereocystis luetkeana): A review of techniques and regional case study. *Global Ecology and Conservation*. 19:e00683. DOI: 10.1016/j.gecco.2019.e00683.

Sibaruddin, H.I., Shafri, H.Z.M., Pradhan, B. & Haron, N.A. 2018. Comparison of pixel-based and object-based image classification techniques in extracting information from UAV imagery data. *IOP Conference Series: Earth and Environmental Science*. 169(1). DOI: 10.1088/1755-1315/169/1/012098.

Smale, D.A., Burrows, M.T., Moore, P., O'Connor, N. & Hawkins, S.J. 2013. Threats and knowledge gaps for ecosystem services provided by kelp forests: A northeast Atlantic perspective. *Ecology and Evolution*. 3(11):4016–4038. DOI: 10.1002/ece3.774.

St-Pierre, A.P. & Gagnon, P. 2020. Kelp-bed dynamics across scales: Enhancing mapping capability with remote sensing and GIS. *Journal of Experimental Marine Biology and Ecology*. 522:151246. DOI: 10.1016/j.jembe.2019.151246.

Stekoll, M.S., Deysher, L.E. & Hess, M. 2006. A remote sensing approach to estimating harvestable kelp biomass. *Journal of Applied Phycology*. 18(3–5):323–334. DOI: 10.1007/s10811-006-9029-7.

Steneck, R.S., Corbett, D., Estes, J.A., Graham, M.H., Bourque, B.J., Tegner, M.J. & Erlandson, J.M. 2002. Kelp forest ecosystems: biodiversity, stability, resilience and future. *Environmental Conservation*. 29:436–459.

Tarr, R.J.Q. 1993. Stock assessment, and aspects of the biology of the South African abalone, Haliotis midae. University of Cape Town. Available: https://open.uct.ac.za/bitstream/handle/11427/26660/Tarr_Stock_assessment_1993_1.pdf?sequence=1&isAllowed=y.

Teagle, H., Hawkins, S.J., Moore, P.J. & Smale, D.A. 2017. The role of kelp species as biogenic habitat formers in coastal marine ecosystems. *Journal of Experimental Marine Biology and Ecology*. 492:81–98. DOI: 10.1016/j.jembe.2017.01.017.

Uhl, F., Bartsch, I. & Oppelt, N. 2016. Submerged kelp detection with hyperspectral data. *Remote Sensing*. 8(6). DOI: 10.3390/rs8060487.

Wernberg, T. & Filbee-Dexter, K. 2019. Missing the marine forest for the trees. *Marine Ecology Progress Series*. 612(1):209–15. DOI: 10.7326/M20-0706.

Appendix A.

A.1 The spectral bands of the S-2 multispectral imagery.

Band Number	Central Wavelength (nm)	Band Name
1	443	Coastal aerosol
2	490	Blue
3	560	Green
4	665	Red
5	705	Vegetation Red Edge
6	740	Vegetation Red Edge
7	783	Vegetation Red Edge
8	842	NIR
8a	865	Narrow NIR
9	945	Water Vapour
10	1380	SWIR – Cirrus
11	1610	SWIR
12	2190	SWIR

Appendix B

B.1 Location of the *Ecklonia maxima* ground truthing points done on the same day as the SAEON HRI capture. The ground-truthing was done by boat by members of Taurus Pty Ltd. At the points viewed in the imagery below, the presence of kelp was confirmed.

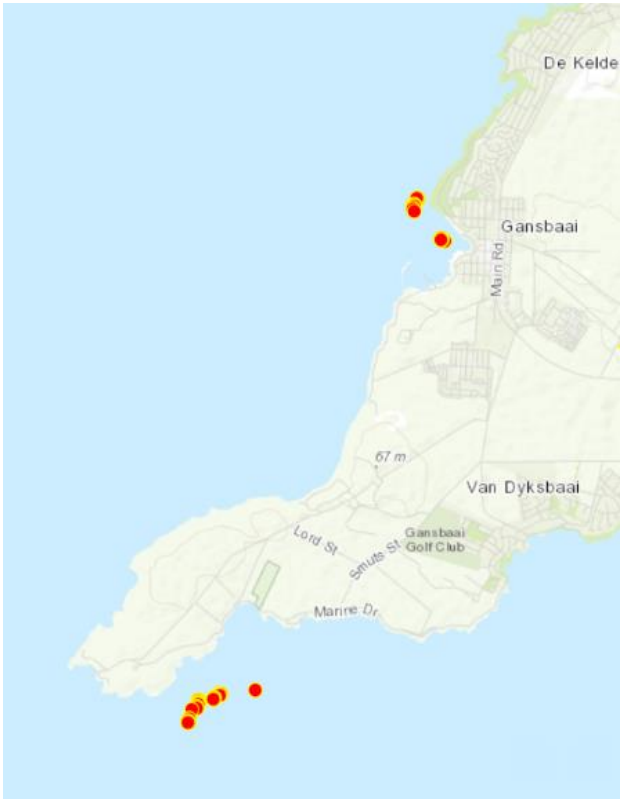

Appendix C

C.1 A zoomed in comparison of the kelp maps at the point of Danger Point Peninsula. With the kelp extent mapped from the high-resolution imagery (A). S2-A kelp extent from this study (B), Dunga (2019) kelp extent (C) Anderson et al. (2007) kelp extent (D), and the raw HRI (E).

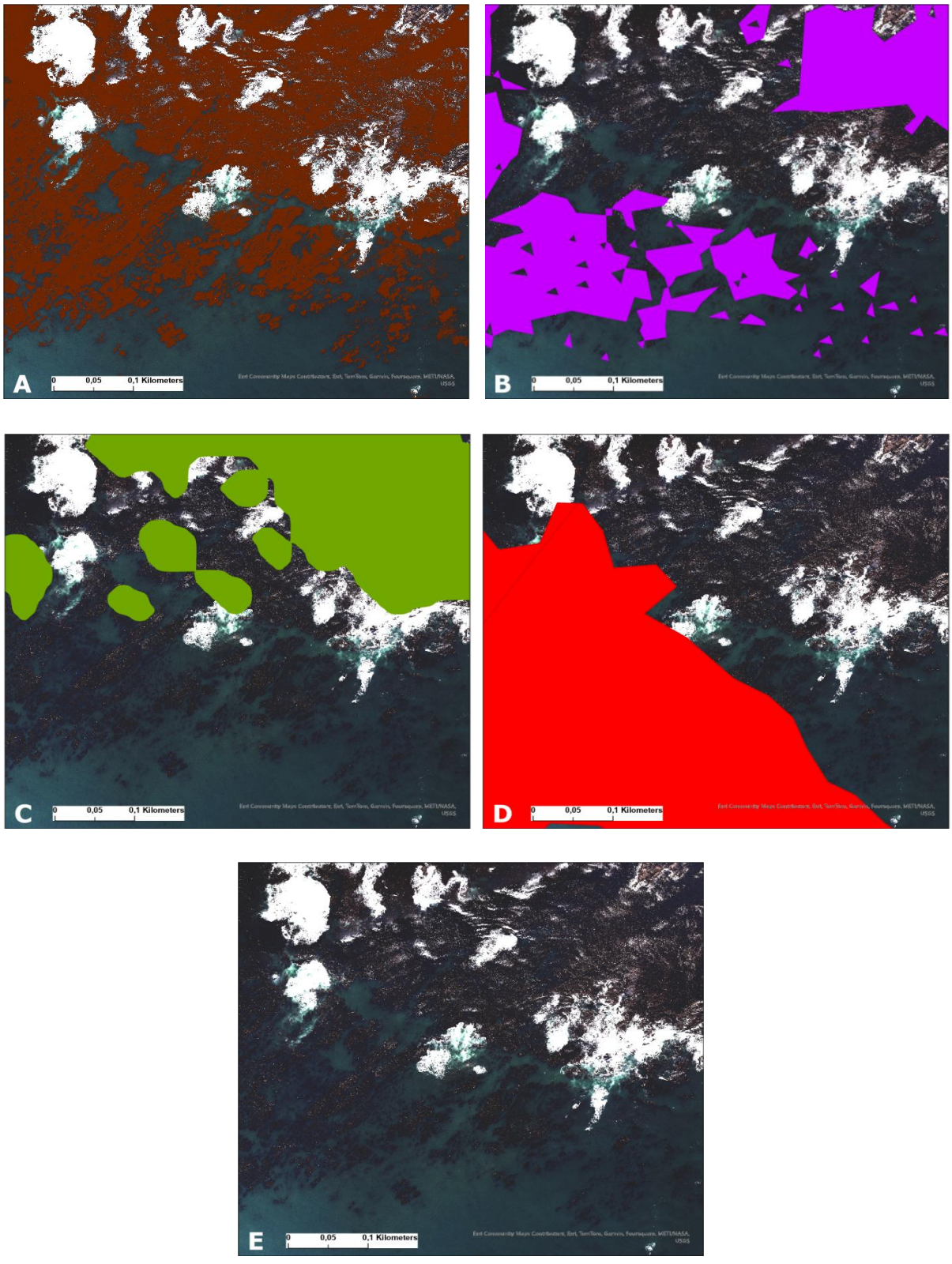

C.2 A zoomed in comparison of the kelp maps North of Gansbaai Harbour. With the kelp extent mapped from the high-resolution imagery (A). S2-A kelp extent from this study (B), Dunga (2019) kelp extent (C) Anderson et al. (2007) kelp extent (D), and the raw HRI (E).